Journal of Anatomy

J. Anat. (2013) **223**, pp641–650 doi: 10.1111/joa.12123

Immunolocalisation of fibrillin microfibrils in the calf metacarpal and vertebral growth plate

Jing Yu and Jill Urban

Department of Physiology, Anatomy and Genetics, University of Oxford, Oxford, UK

Abstract

Overgrowth of limbs and spinal deformities are typical clinical manifestations of Marfan syndrome (MFS) and congenital contractural arachnodactyly (CCA), caused by mutations of the genes encoding fibrillin-1 (FBN1) and fibrillin-2 (FBN2), respectively. FBN1 mutations are also associated with acromicric (AD) and geleophysic dysplasias (GD), and with Weill–Marchesani syndrome (WMS), which is characterised by short stature. The mechanisms leading to such abnormal skeletal growth and the involvement of the fibrillins are not understood. Postnatal longitudinal bone growth mainly occurs in the epiphyseal growth plate. Here we investigated the organisation of fibrillin microfibrils in the growth plate of the long bone and vertebra immunohistochemically. Fibrillin-1 was dual-immunostained with elastin, with fibrillin-2 or with collagen X. We report that fibrillin microfibrils are distributed throughout all regions of the growth plate, and that fibrillin-1 and fibrillin-2 were differentially organised. Fibrillin-1 was more abundant in the extracellular matrix of the resting and proliferative zones of the growth plate than in the hypertrophic zone. More fibrillin-2 was found in the calcified region than in the other regions. No elastin fibres were observed in either the proliferative or hypertrophic zones. This study indicates that, as fibrillin microfibrils are involved in growth factor binding and may play a mechanical role, they could be directly involved in regulating bone growth. Hence, mutations of the fibrillins could affect their functional role in growth and lead to the growth disorders seen in patients with MFS, CCA, AD, GD and WMS.

Key words: congenital contractural arachnodactyly; elastin; epiphyseal growth plate; fibrillin-1; fibrillin-2; Marfan syndrome; Weill–Marchesani syndrome.

Introduction

Human postnatal long bone growth occurs in the epiphyseal growth plate located between the epiphysis and diaphysis of the long bones (reviewed by Kronenberg, 2003; Mackie et al. 2011); the mechanism of vertebral body growth in height is similar to that in long bones (Haas, 1939; Dickson & Deacon, 1987), but less well studied. During endochondral growth, cells undergo a differentiation cycle, progressing from resting cells through a proliferating stage to a final stage of hypertrophy terminating in apoptotic cell death (Wilsman et al. 1996). Three distinct zones in the epiphyseal growth plate, defined as resting (RZ), proliferation (PZ) and hypertrophic (HZ), can be distinguished by differences in cell morphology, matrix composition and cell metabolism (Hunziker et al. 1987; Farnum, 1994). Cellular activities in the different zones are closely regulated by complex interactions between several systems, including the endocrine system (Nilsson et al. 2005; Shao et al. 2006), locally produced growth factors (Kronenberg, 2003) and mechanical signalling (Stokes et al. 2006, 2007; Foolen et al. 2011). The composition and organisation of extracellular matrix (ECM) proteins (Byers et al. 1992; Yamasaki et al. 2001; Melrose et al. 2003) also appears important in growth regulation with mutations in a number of different ECM components, such as cartilage oligomeric protein and collagen IX leading to multiple epiphyseal dysplasia and pseudoachondroplasia and other growth disorders (Bateman et al. 2009).

The role of the fibrillins has, however, been little explored. Fibrillin-1 has been found in other cartilages (Keene et al. 1997; Yu & Urban, 2010), but the presence of fibrillins in the growth plate has not been documented to date, even though mutations of the genes encoding fibrillin-1 and fibrillin-2 lead to growth disturbances. Overgrowth of limbs and scoliosis are characteristics of patients with Marfan syndrome (MFS; OMIM: 154700) or congenital contractural arachnodactyly (CCA; OMIM: 121050), arising from mutations of FBN1 and FBN2, respectively (Gupta et al. 2002; Judge & Dietz, 2005; Al Kaissi et al. 2013). Mutations in the FBN1 gene have also been found in patients

Correspondence
Jing Yu, Department of Physiology, Anatomy and Genetics, University of Oxford, Oxford OX1 3PT, UK. T: +44 1865 272479; F: +44 1865 272369; E: jing.yu@dpag.ox.ac.uk

Accepted for publication *10 September 2013*
Article published online *9 October 2013*

with the opposite phenotype to those of patients with MFS, such as patients with geleophysic dysplasia (GD; OMIM: 231050) and acromicric dysplasia (AD; OMIM: 102370), and with Weill–Marchesani syndrome (WMS; OMIM: 608328; Faivre et al. 2003; Le Goff et al. 2011; Sengle et al. 2012), all characterised by severely short stature. How fibrillins and their mutations influence long bone growth is, however, poorly understood.

Fibrillin microfibrils are associated with the elastic fibre network, which in general consists of an elastin core surrounded by a network of fibrillin microfibrils. An extensive elastic network is distributed in the ECM of many tissues (Ramirez et al. 2004; Olivieri et al. 2010), such as skin, lung and blood vessels. In some tissues, such as the eye ciliary zonule (Streeten & Licari, 1983; Sherratt et al. 2003), only the microfibrillar proteins are present. Until relatively recently, the major role of the fibrillin microfibrils together with elastin as the elastic fibre network was thought to be mechanical, providing resilience and promoting tissue recovery from deformation (Kielty et al. 2002). However, recently microfibrils have been shown to sequester growth factors, particularly those of the transforming growth factor TGF-beta superfamily, and appear important in regulating the activity of bone morphogenetic proteins (BMPs) and TGF-beta, which both play a role in bone growth (Charbonneau et al. 2004; Al Kaissi et al. 2013).

FBN1 mutations leading to the short-stature found in GD, AD and WMS result in disturbances in microfibril formation, and are also all located in regions of the gene associated with TGF-beta binding (Faivre et al. 2003; Le Goff et al. 2011). Hence, we suggest that if present in the growth plate, the microfibril system could influence bone growth by regulating mechanical forces and/or by sequestering growth factors. The aim of this study is thus to investigate the distribution of fibrillin-1 and fibrillin-2 and the associated elastin network in the growth plate, and thus to further understanding of whether fibrillin microfibrils might play a role in normal and pathological bone growth.

Materials and methods

Tissue preparation

Five fresh metacarpal–phalangeal joints and tails from 7-day-old calves were collected from a local abattoir. The metacarpal and vertebral joints were dissected (Fig. 1) and immediately stored at −80 °C till used. The joints were then defrosted at room temperature, further sagittally dissected (Fig. 1) and specimens then snap frozen. Cryostat sections, 20 μm thickness, were cut and mounted on super-frosted slides and stored at −20 °C till further analysed. Figure 1 illustrates the specimen preparation.

H&E staining

Conventional H&E staining (http://protocolsonline.com/histology/haematoxylin-eosin-he-staining/) was used to study general tissue structure and cell organisation.

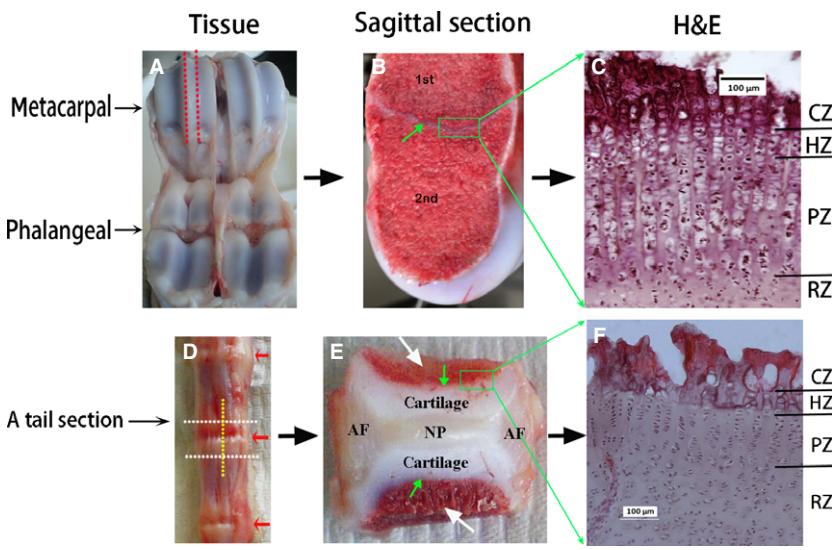

Fig. 1 Specimen preparation. (A-C) Metacarpal joint. (A) Calf metacarpal-phalangeal joint. Red dashed lines indicate where specimen was sagittally dissected. (B) Sagittally dissected specimen, green arrow highlights the growth plate separating the primary (1st) and secondary (2nd) ossification centres. Green square highlights growth plate specimen dissected out for histology. (C) H&E stained micrograph of the metacarpal growth plate. (D-F) Vertebral joint. (D) Calf tail joints. The vertebral joint was dissected through the white dashed lines, then sagittally dissected along the yellow dashed line. Red arrows indicate the intervertebral discs. (E) A mid-sagittal dissected specimen, illustrating the general structure of a vertebral joint composed of the disc nucleus pulposus (NP) in the centre surrounded laterally by the disc annulus fibrosus (AF), longitudinally by cartilages which directly attached to the vertebral bone (white arrows) though the growth plate (green arrows). Green square highlights growth plate specimen dissected out for histology. (F) H&E stained micrograph of the vertebral growth plate. RZ, resting zone; PZ, proliferative zone; HZ, hypertrophic zone; CZ, calcified region of the hypertrophic zone.

Immunofluorescence staining

The elastic fibre network is better visualised immunohistologically after treating tissue sections with hyaluronidase or collagenase (Yu et al. 2002, 2007) to partially remove the masking effect of tissue matrix proteins. Here we investigated various predigestion methods, including hyaluronidase pre-treatment for 2 h or overnight (15 h) at 37 °C or collagenase pre-treatment for 30 min at 37 °C, and compared results with no pre-treatment (not shown). Pre-treating defrosted specimens with hyaluronidase (Sigma H6254, concentration of 4800 U mL^{-1}) at 37 °C overnight before immunostaining was found to be sufficient and was mainly used for this study.

Unfixed sections were then dual-immunostained with fibrillin-1 together with elastin, collagen X or fibrillin-2. Table 1 lists the primary and secondary antibodies used.

Details of the dual-immunostaining methods used have been described previously (Yu et al. 2007). Briefly, fresh and pre-treated sections were washed with Tris buffer (50 mM Tris-HCl + 10 mM calcium acetate, pH 7.2) and blocked with 10% normal donkey serum (in Tris buffer). Sections were then incubated with primary anti-bovine fibrillin-1 mouse monoclonal antibody at 4 °C overnight. After washing with phosphate-buffered saline (PBS), sections were then incubated with the donkey anti-mouse antibody conjugated with Cy3 at room temperature for 45 min. After washing again with PBS, sections were then blocked with 10% normal donkey serum, then incubated with either primary anti-elastin or anti-collagen X or anti-fibrillin-2 rabbit polyclonal antibody at 4 °C overnight. The sections were then washed with PBS, and then incubated with donkey anti-rabbit antibody conjugated with dylight-488 at room temperature for 45 min. Sections were then washed and mounted with mounting medium (Vector Laboratory, Cat No: H1500).

Microscopy and image processing

All sections were examined using a conventional fluorescence microscope (Leica DMRB) combined with a phase contrast filter. Several sequential images of the same site were taken manually without moving the slides, either by changing the focus to track the fibres or by switching to different filters keeping the same focus. Images were then processed with ADOBE PHOTOSHOP CS5. In order to improve contrast of the dual-immunostained fluorescent dyes, images of Cy3-labelled fibrillin-1 were changed to red using the same software. Multiple images from the same specimen site were merged together (layers option) using the same software.

Results

General structure and morphology

Metacarpal–phalangeal joint and growth plate

The second ossification centre was well developed in all metacarpal bones examined (Fig. 1B). The different zones of the metacarpal growth plate (Fig. 1C) based on the cell organisation and appearance were evident, i.e. RZ, PZ, HZ, and the calcified region of the hypertrophic zone (CZ).

A vertebral joint and growth plate

In the calf tail used, the second ossification centre was only seen in the first three proximal joints along the axis of the calf tail. Before the formation of its second ossification centre, a young vertebral joint in the more distal region of the tail, (Fig. 1E) is composed of the intervertebral disc flanked longitudinally by cartilages that are connected to the adjacent vertebral bodies (white arrows) through the growth plate (green arrows). As in the growth plate of a long bone, the growth plate of the developing vertebra appeared composed by distinct zones, defined by their appearance and by cell organisation (Fig. 1F), viz. the RZ, the PZ, HZ and CZ.

Table 1 List of antibodies used.*

	Primary antibody	Secondary antibody
Fibrillin-1	Mouse anti-bovine fibrillin-1 from Abcam UK Ltd, UK, Cat. No: ab3090 Dilution: 1 : 50 Buffer: 50 mM Tris-HCl plus 10 mM calcium acetate	Cy3-conjugated donkey anti-mouse IgG from Stratech Scientific Ltd, UK, (Red) Cat. No: 715-165-151 Dilution: 1 : 100
Elastin	Rabbit anti-human α-elastin antibody (cross-reacting with bovine) from AbDserotec, UK, Cat. No: 4060-1054, Batch No: 20092751 Dilution: 1 : 50	Dylight-488 conjugated donkey anti-rabbit IgG from Stratech Scientific Ltd, UK (Green) Cat. No: 712-485-153 Dilution: 1 : 100
Fibrillin-2	Rabbit anti-human fibrillin-2 antibody (cross-reacting with bovine) from Elastin Products Company, USA, Cat. No: PR225 Dilution: 1 : 50	As above
Collagen X	Rabbit anti-rat collagen X antibody (cross-reacting with bovine) from Abcam UK, Cat. No: ab58632 Dilution: 1 : 50	As above

*Antibodies are diluted with PBS, unless otherwise indicated.

The cell columns of the HZ and PZ of the vertebral growth plates were, however, typically shorter than those of the metacarpal growth plates.

Organisation of fibrillin microfibrils in the metacarpal growth plate

Typical images of a metacarpal growth plate immunostained for fibrillin-1 are shown in Fig. 2; the microfibrils could be visualised in all the regions of the growth plate. They were not only apparent in the ECM of the RZ of the cartilage, as reported previously (Keene et al. 1997), but we observed an extensive network of fibrillin-1 microfibrils also in the ECM of the PZ and HZ where they appeared to form columns encircling the cells (white arrows in Fig. 2B). This fibrillin-1 network seems stained more intensely in the PZ region than in the HZ region. In order to clarify differences in zonal distribution, dual-immunostaining of fibrillin-1 with collagen X was carried out; typical results are shown in Fig. 3. Collagen X is mainly expressed in the HZ (Schmid & Linsenmayer, 1985), therefore it can be used as a marker for the HZ region. If Fig. 3B is compared with Fig. 3C, it can be seen that fibrillin-1 stained more intensely in the PZ region than that in the HZ region. The merged image (3D) further confirmed the finding.

As mentioned above, mutations in the genes encoding fibrillin-1 or fibrillin-2 lead to MFS or CCA, respectively. Both syndromes share some similar features, viz. elongated fingers and limbs, and also scoliosis. Therefore, dual-immunostaining of fibrillin-1 and fibrillin-2 was carried out, typical results are shown in Fig. 4. Relatively little fibrillin-2 staining was visible in the PZ and HZ regions (Fig. 4B), and also little was apparent in the RZ (not shown). Fibrillin-2, however, was more evident in the calcified zone, where fibrillin-1 was also seen (compare Fig. 4B with Fig. 4C).

Organisation of fibrillin microfibrils in the vertebral growth plate

Figure 5 shows typical results of immunostaining fibrillin-1 in the growth plate of the calf tail. As seen in the metacarpal growth plate (Fig. 2), immunostained fibrillin-1 was apparent in all regions of the vertebral growth plate, with stronger staining in the ECM of the RZ and PZ (Fig. 5B,E), and relatively less staining in the HZ and CZ regions. As above, in order to clarify the zonal distribution, dual-

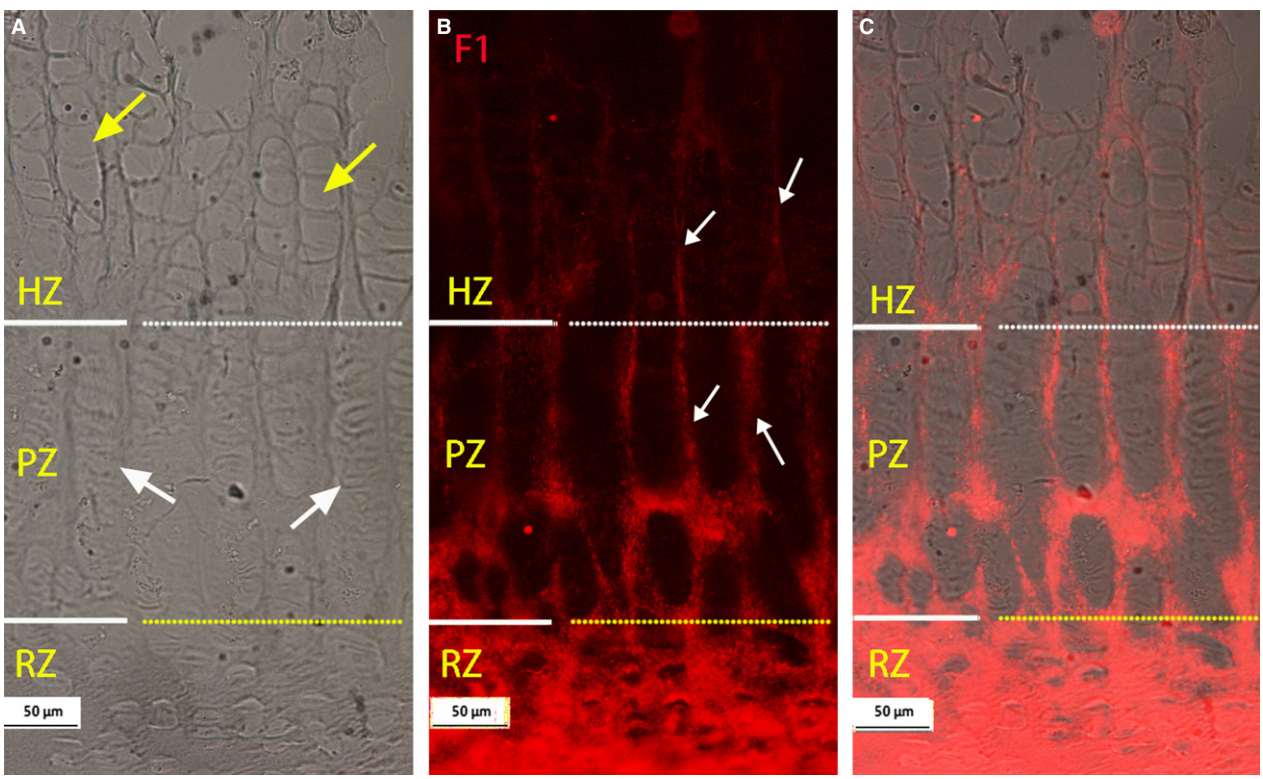

Fig. 2 Typical distribution of microfibrils immunostained with fibrillin-1 (F1) (red) in the metacarpal growth plate. (A-B) Micrographs from same site; dashed white and yellow lines separates the HZ from the PZ and the PZ from the RZ. (A) Phase contrast image, yellow and white arrows indicate typical hypertrophic and proliferative cell columns respectively. (B) Microfibrils immunostained with F1, visible in all zones of the growth plate, with relatively intense staining in the RZ and PZ regions and less staining in the HZ region. At the PZ and HZ, microfibrils appear encircling cell columns (highlighted with white arrows). (C) Merged image of A and B. RZ, resting zone; PZ, proliferative zone; HZ, hypertrophic zone.

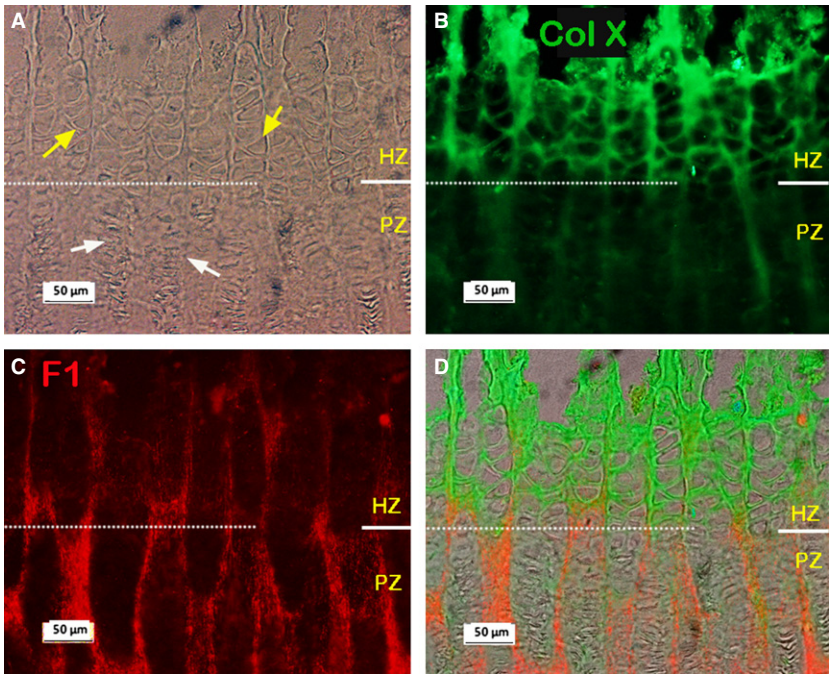

Fig. 3 Typical dual-immunostained collagen X (Col X; green) and fibrillin-1 (F1; red) in the metacarpal growth plate. (A-C) Micrographs from same site, white dashed line separates the HZ and PZ regions. (A) Phase contrast image. (B) Immunostained collagen X (Col X) showing strong staining for Col X in the HZ region. (C) Immunostained F1 showing relatively more F1 in the PZ than in HZ regions. (D) Merged image of A, B and C. RZ, resting zone; PZ, proliferative zone; HZ, hypertrophic zone.

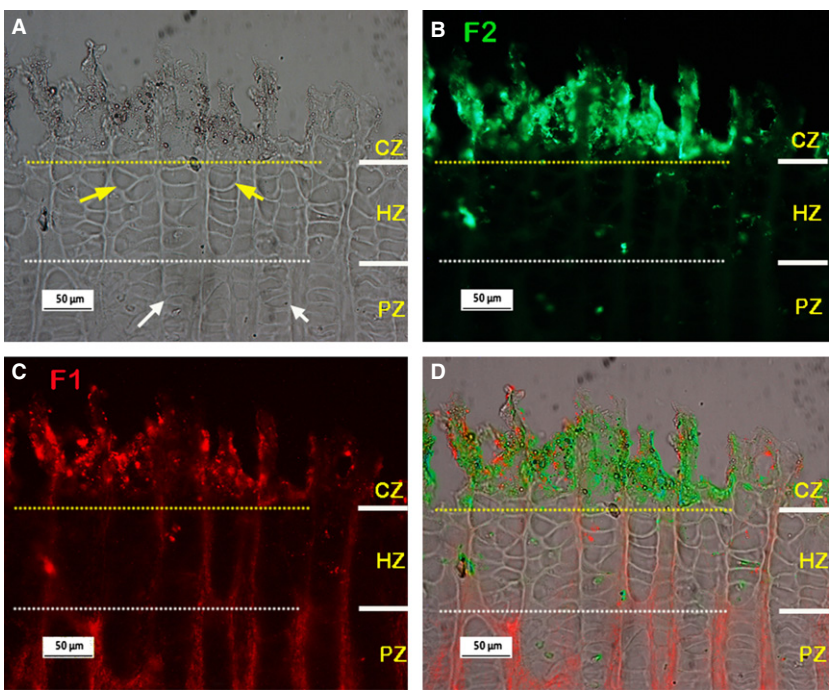

Fig. 4 Typical dual-immunostained fibrillin-1 (F1; red) and fibrillin-2 (F2; green) in the metacarpal growth plate (pre-treatment condition: hyaluronidase 2hrs at 37°C; longer incubation in hyaluronidase can lead to loosening and loss of the calcified tissue). (A-C) Micrographs from the same site, yellow and white dashed lines separating the CZ from the HZ and the HZ from the PZ regions respectively. (A) Phase contrast image, white and yellow arrows indicate typical proliferative and hypertrophic cell columns respectively. (B-C) Immunostained F2 and F1 respectively, showing little F2 staining is visible in the HZ and PZ regions but strong staining for F2 is apparent in the CZ where F1 is also apparent. (D) Merged images of A-C. RZ, resting zone; PZ, proliferative zone; HZ, hypertrophic zone; CZ, calcified region of the hypertrophic zone.

immunostaining of collagen X with fibrillin-1 was carried out. The results confirmed that fibrillin-1 was present in the HZ region, but that staining was less intense there than in other zones (Fig. 6). Dual-immunostaining of fibrillin-1 and fibrillin-2 showed stronger staining of fibrillin-2 (Fig. 7C,H) than seen in the metacarpal growth plate (Fig. 4B), with relatively more fibrillin-2 distributed in the HZ, and less in the PZ and RZ compared with fibrillin-1, the two highly coloca-

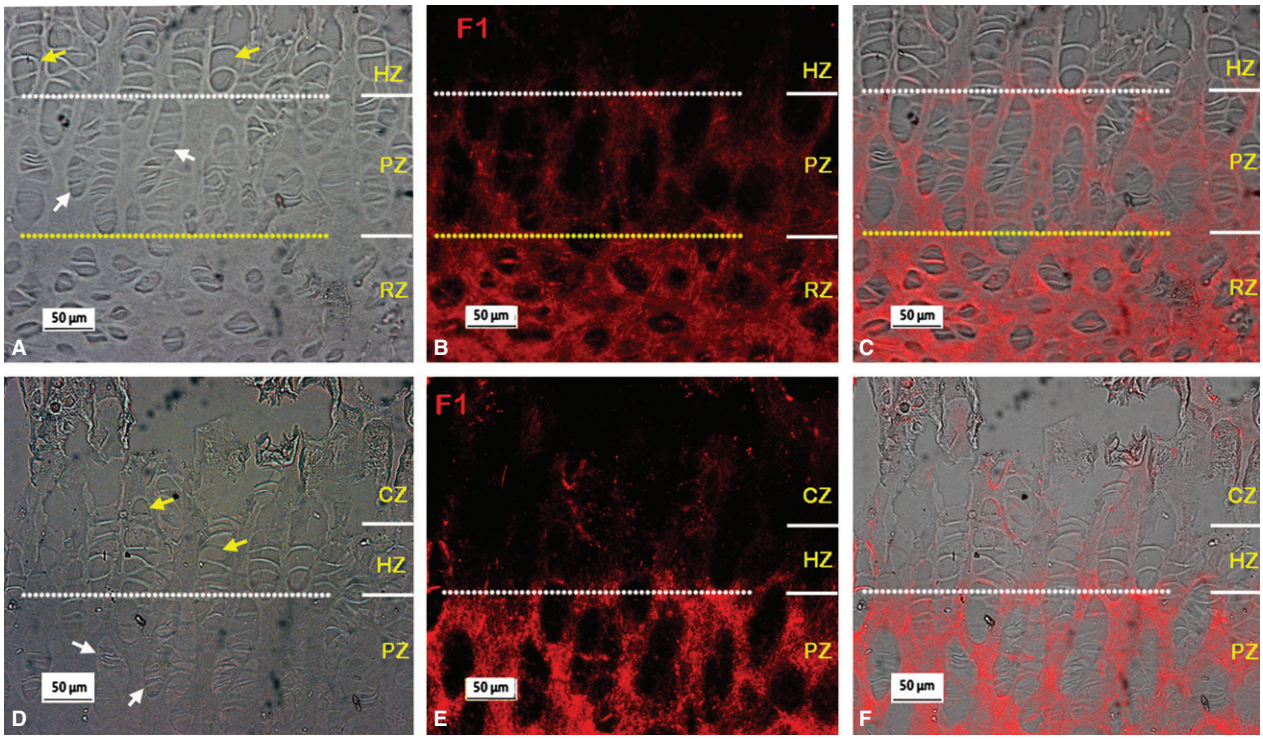

Fig. 5 Typical fibrillin-1 (F1) microfibril organisation in the vertebral growth plate. A,B and D,E are micrographs took from the same sites respectively. (A,D) Phase contrast images showing the organisation of cells in the vertebral growth plate; hypertrophic and proliferative zone cells are highlighted with yellow and white arrows respectively. (B,E) Immunostained fibrillin-1 images from the identical areas of A and D respectively, showing extensive fibrillin-1 staining in the resting zone (RZ) and relatively more F1 staining in the proliferative zone (PZ) than that in the hypertrophic zone (HZ). CZ, calcified region of the hypertrophic zone.

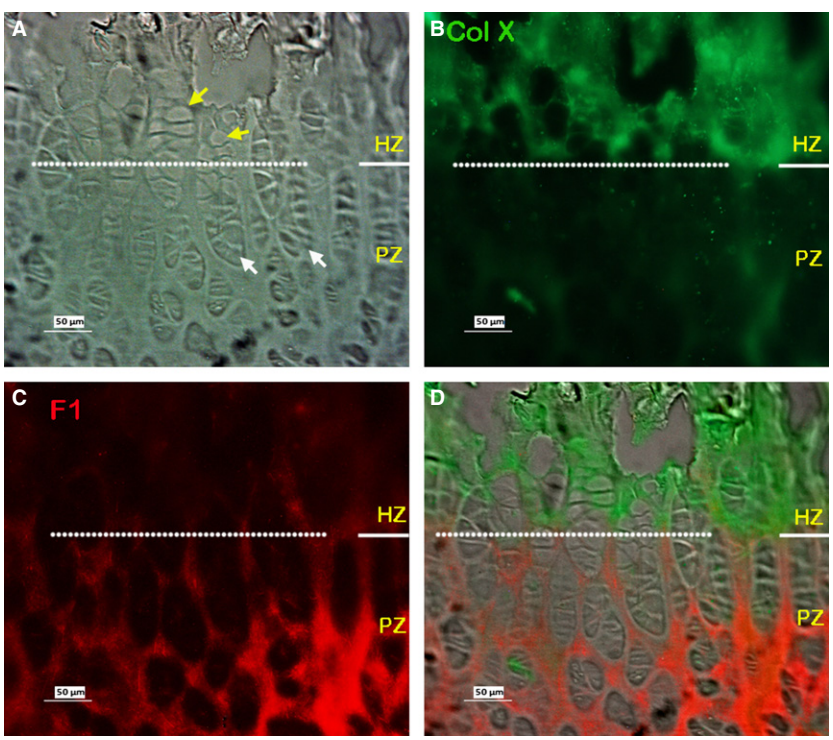

Fig. 6 Typical dual-immunostained Collagen X (Col X; green) and fibrillin-1 (F1; red) in the vertebral growth plate. (A-C) Images are micrographs from the same site. (A) Phase contrast image. (B) Immunostained collagen X (ColX), mainly visible in the HZ as previously reported. (C) Immunostained fibrillin-1, showing fibrillin-1 microfibrils more apparent in the PZ than the HZ as seen in Fig 5. (D) Merged image of B and C. (E) Merged image of A-C. PZ, proliferative zone; HZ, hypertrophic zone.

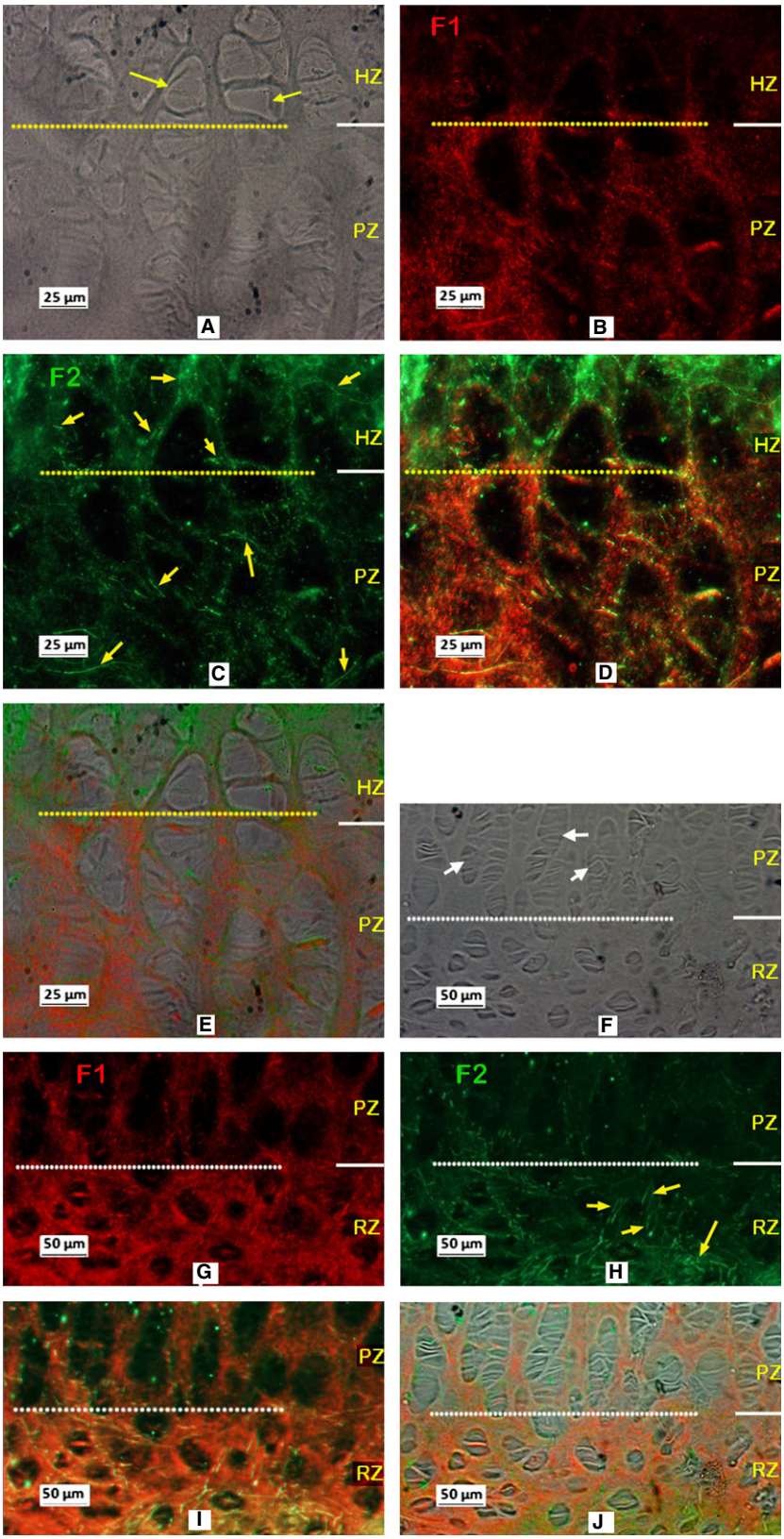

Fig. 7 Typical dual-immunostained fibrillin-1 (F1; red) and fibrillin-2 (F2; green) in the vertebral growth plate. A to C, E to G are micrographs are took from the same site of a section respectively. (A,E) Under phase contrast, white and yellow arrows indicating the typical proliferating and hypertrophy cells respectively. B,C and F,G are the micrographs of dual-immunostained fibrillin-1 and fibrillin-2 respectively, showing F2 apparent in all three zones of the growth plate, highlighted with yellow arrows in C and G. (D,H) Merged image of B,C and F,G respectively showing relatively more fibrillin-2 in the HZ, and less in the PZ and RZ compared to fibrillin-1, the two highly colocalised otherwise. RZ, resting zone; PZ, proliferative zone; HZ, hypertrophic zone.

lised otherwise (Fig. 7D,I). As in the metacarpal growth plate (Fig. 4), fibrillin-2 staining was most intense in the calcified zone (not shown).

Elastin was not observed in the PZ and HZ of either the metacarpal–phalangeal or vertebral growth plates. Extensive staining for elastin was, however, observed in the RZ of

vertebral growth plate (not shown), but not in the metacarpal–phalangeal growth plate.

Discussion

Here we report that fibrillin microfibrils are distributed throughout all the regions of the 7-days calf metacarpal and vertebral growth plates.

An extensive network of fibrillin-1 was seen in the ECM of the RZ and PZ of the vertebral and metacarpal growth plates (Figs 2B, 3C, 5B,E, 6C,7B,G), but fibrillin-1 was relatively sparsely distributed in the HZ. Dual-immunostaining of collagen X with fibrillin-1 further confirmed zonal fibrillin-1 distribution (Figs 3 and 6). By contrast, staining of the fibrillin-2 network was most intense in the calcified zone (Fig. 4), with relatively more fibrillin-2 found in the HZ of the vertebral growth plate than fibrillin-1 (Fig. 7). No elastin fibres were seen in the PZ and HZ.

The extensive organisation of fibrillin microfibrils in different regions of the growth plate suggests the network of microfibrils could play a functional role in the long bone and spinal growth. Microfibrils, as part of the elastic fibre system, are commonly thought to play a mechanical role. Even though elastin was not observed in the ECM surrounding the cell columns of the growth plate, microfibrils alone could play a mechanical role as seen in the ocular zonules (Streeten & Licari, 1983; Sherratt et al. 2003). The growth rate and organisation of the growth plate is sensitive to inappropriate external mechanical loading (Roaf, 1960; Farnum & Wilsman, 1993; Stokes et al. 2005, 2006, 2007), to tension imposed by the periosteum (Foolen et al. 2011) and to disruptions of ECM organisation (Blumbach et al. 2008; Plumb et al. 2011). The organisation of the fibrillins in the growth plate suggests their networks could play a mechanical role. There is further support for this suggestion from observations of disturbed fibrillin organisation in disorders arising from FBN1 mutations.

Over 600 mutations of FBN1 have been associated with MFS (UMD-FBN1; http:/www.umd.be) leading to tall stature and long limbs, even though genotype–phenotype correlations have, in the main, been poorly established (Faivre et al. 2003; Mizuguchi & Matsumoto, 2007). However, FBN1 mutations that abolish binding to ADAMTSLIKE (ADAMTSL) proteins (Sengle et al. 2012) or mutations of TGF-beta binding protein-like 5 domain in fibrillin-1 appear to lead to GD, AD (Le Goff et al. 2011) or WMS (Faivre et al. 2003), characterised by short stature. Interestingly, mutations in ADAMTSL2 and ADAMTS10 were found to be associated with GD (Le Goff et al. 2008) and a recessive form of WMS (Dagoneau et al. 2004), respectively. Results suggest that a complex formed from specific ADAMTS and ADAMTSL proteins binds to FBN1, influences fibrillin-1 microfibril formation and hence fibrillin-1 function (Le Goff et al. 2011; Sengle et al. 2012). Microfibrils formed from cells of patients with WMS, AD, GD and MFS are irregular and disorganised *in situ* compared with controls (Hollister et al. 1990; Le Goff et al. 2011; Sengle et al. 2012). Such differences in microfibril formation could influence mechanotransduction in the growth plate and hence bone growth (Sengle et al. 2012).

More recently, fibrillins have also been shown to regulate the bioavailability of TGF-betas and BMPs (reviewed by Ramirez & Rifkin, 2009; Ramirez & Sakai, 2010). Growth factors of the TGF-beta family are targeted to microfibrils indirectly through the latent TGF-beta binding proteins 1,3,4 (LTBPs; Rifkin, 2005; Ramirez & Rifkin, 2009). These LTBPs are able to bind to fibrillin-1 and fibrillin-2 *in vitro*, and co-localise with microfibrils *in vivo* (Isogai et al. 2003). BMPs can directly target to microfibrils (both fibrillin-1 and fibrillin-2) through their pro-domains (Gregory et al. 2005; Sengle et al. 2008, 2011). The TGF-beta and BMP-family proteins, their associated receptors and their transcription factors, the Smads, are expressed in all the regions of the growth plate (Yazaki et al. 1998; Sakou et al. 1999; Keller et al. 2011). The patterns of expression of their transcription factors, the Smads, and studies on transgenic mice indicate that TGF-betas and BMPs play different temporal and spatial roles in regulating postnatal vertebral body growth, and that there is considerable interaction between them (Bailon-Plaza et al. 1999; Dahia et al. 2011; Keller et al. 2011). As TGF-beta and BMPs appear to be modulated differentially by fibrillin-1 and fibrillin-1 during bone formation *in vitro* (Nistala et al. 2010), the specific organisation of these microfibrils within the growth plate may have a role in the differential regulation of activity of these growth factors. FBN1 mutations could also affect TGF-beta signalling (Neptune et al. 2003; Le Goff et al. 2011; Sengle et al. 2012). Indeed, upregulation of TGF-beta secretion has been shown in MFS (Neptune et al. 2003; Habashi et al. 2006) and GD and AD (Habashi et al. 2006; Le Goff et al. 2011), but not in WMS (Sengle et al. 2012). How these changes in fibril organisation and TGF-beta expression lead to the opposite skeletal phenotypes seen in MFS, WMS, GD and AD is unknown at present.

In summary, this study reports that fibrillin microfibrils form an extensive network in the ECM of the growth plate indicating direct involvement of fibrillin-1 and fibrillin-2 in bone growth.

Acknowledgements

This work was supported financially by the British Scoliosis Foundation and by the European Community's Seventh Framework Programme (FP7, 2007–2013) under grant agreement no. HEALTH-F2-2008-201626.

References

Al Kaissi A, Zwettler E, Ganger R, et al. (2013) Musculo-skeletal abnormalities in patients with Marfan syndrome. *Clin Med Insights Arthritis Musculoskelet Disord* **6**, 1–9.

Bailon-Plaza A, Lee AO, Veson EC, et al. (1999) BMP-5 deficiency alters chondrocytic activity in the mouse proximal tibial growth plate. *Bone* **24**, 211–216.

Bateman JF, Boot-Handford RP, Lamande SR (2009) Genetic diseases of connective tissues: cellular and extracellular effects of ECM mutations. *Nat Rev Genet* **10**, 173–183.

Blumbach K, Niehoff A, Paulsson M, et al. (2008) Ablation of collagen IX and COMP disrupts epiphyseal cartilage architecture. *Matrix Biol* **27**, 306–318.

Byers S, Caterson B, Hopwood JJ, et al. (1992) Immunolocation analysis of glycosaminoglycans in the human growth plate. *J Histochem Cytochem* **40**, 275–282.

Charbonneau NL, Ono RN, Corson GM, et al. (2004) Fine tuning of growth factor signals depends on fibrillin microfibril networks. *Birth Defects Res C Embryo Today* **72**, 37–50.

Dagoneau N, Benoist-Lasselin C, Huber C, et al. (2004) ADAMTS10 mutations in autosomal recessive Weill-Marchesani syndrome. *Am J Hum Genet* **75**, 801–806.

Dahia CL, Mahoney EJ, Durrani AA, et al. (2011) Intercellular signaling pathways active during and after growth and differentiation of the lumbar vertebral growth plate. *Spine (Phila Pa 1976)* **36**, 1071–1080.

Dickson RA, Deacon P (1987) Spinal growth. *J Bone Joint Surg* **69**, 690–692.

Faivre L, Gorlin RJ, Wirtz MK, et al. (2003) In frame fibrillin-1 gene deletion in autosomal dominant Weill-Marchesani syndrome. *J Med Genet* **40**, 34–36.

Farnum CE. (1994). Differential growth rates of long bones. In: *Bone*. (ed. Hall B), pp. 193–222. Boca Raton:CRC Press.

Farnum CE, Wilsman NJ (1993) Determination of proliferative characteristics of growth plate chondrocytes by labeling with bromodeoxyuridine. *Calcif Tissue Int* **52**, 110–119.

Foolen J, van Donkelaar CC, Ito K (2011) Intracellular tension in periosteum/perichondrium cells regulates long bone growth. *J Orthop Res* **29**, 84–91.

Gregory KE, Ono RN, Charbonneau NL, et al. (2005) The prodomain of BMP-7 targets the BMP-7 complex to the extracellular matrix. *J Biol Chem* **280**, 27 970–27 980.

Gupta PA, Putnam EA, Carmical SG, et al. (2002) Ten novel FBN2 mutations in congenital contractural arachnodactyly: delineation of the molecular pathogenesis and clinical phenotype. *Hum Mutat* **19**, 39–48.

Haas SL (1939) Growth in length of vertebrae. *Arch Surg* **38**, 245–249.

Habashi JP, Judge DP, Holm TM, et al. (2006) Losartan, an AT1 antagonist, prevents aortic aneurysm in a mouse model of Marfan syndrome. *Science (New York, NY)* **312**, 117–121.

Hollister DW, Godfrey M, Sakai LY, et al. (1990) Immunohistologic abnormalities of the microfibrillar-fiber system in the Marfan syndrome. *The New England Journal of Medicine* **323**, 152–159.

Hunziker EB, Schenk RK, Cruz-Orive LM (1987) Quantitation of chondrocyte performance in growth-plate cartilage during longitudinal bone growth. *J Bone Joint Surg Am* **69**, 162–173.

Isogai Z, Ono RN, Ushiro S, et al. (2003) Latent transforming growth factor beta-binding protein 1 interacts with fibrillin and is a microfibril-associated protein. *J Biol Chem* **278**, 2750–2757.

Judge DP, Dietz HC (2005) Marfan's syndrome. *Lancet* **366**, 1965–1976.

Keene DR, Jordan CD, Reinhardt DP, et al. (1997) Fibrillin-1 in human cartilage: developmental expression and formation of special banded fibers. *J Histochem Cytochem* **45**, 1069–1082.

Keller B, Yang T, Chen Y, et al. (2011) Interaction of TGFbeta and BMP signaling pathways during chondrogenesis. *PLoS ONE* **6**, e16421.

Kielty CM, Sherratt MJ, Shuttleworth CA (2002) Elastic fibres. *J Cell Sci* **115**, 2817–2828.

Kronenberg HM (2003) Developmental regulation of the growth plate. *Nature* **423**, 332–336.

Le Goff C, Morice-Picard F, Dagoneau N, et al. (2008) ADAMTSL2 mutations in geleophysic dysplasia demonstrate a role for ADAMTS-like proteins in TGF-beta bioavailability regulation. *Nat Genet* **40**, 1119–1123.

Le Goff C, Mahaut C, Wang LW, et al. (2011) Mutations in the TGFbeta binding-protein-like domain 5 of FBN1 are responsible for acromicric and geleophysic dysplasias. *Am J Hum Genet* **89**, 7–14.

Mackie EJ, Tatarczuch L, Mirams M (2011) The skeleton: a multifunctional complex organ: the growth plate chondrocyte and endochondral ossification. *J Endocrinol* **211**, 109–121.

Melrose J, Smith S, Ghosh P, et al. (2003) Perlecan, the multidomain heparan sulfate proteoglycan of basement membranes, is also a prominent component of the cartilaginous primordia in the developing human fetal spine. *J Histochem Cytochem* **51**, 1331–1341.

Mizuguchi T, Matsumoto N (2007) Recent progress in genetics of Marfan syndrome and Marfan-associated disorders. *J Hum Genet* **52**, 1–12.

Neptune ER, Frischmeyer PA, Arking DE, et al. (2003) Dysregulation of TGF-beta activation contributes to pathogenesis in Marfan syndrome. *Nat Genet* **33**, 407–411.

Nilsson O, Marino R, De Luca F, et al. (2005) Endocrine regulation of the growth plate. *Horm Res* **64**, 157–165.

Nistala H, Lee-Arteaga S, Smaldone S, et al. (2010) Fibrillin-1 and -2 differentially modulate endogenous TGF-beta and BMP bioavailability during bone formation. *J Cell Biol* **190**, 1107–1121.

Olivieri J, Smaldone S, Ramirez F (2010) Fibrillin assemblies: extracellular determinants of tissue formation and fibrosis. *Fibrogenesis Tissue Repair* **3**, 24.

Plumb DA, Ferrara L, Torbica T, et al. (2011) Collagen XXVII organises the pericellular matrix in the growth plate. *PLoS ONE* **6**, e29422.

Ramirez F, Rifkin DB (2009) Extracellular microfibrils: contextual platforms for TGFbeta and BMP signaling. *Curr Opin Cell Biol* **21**, 616–622.

Ramirez F, Sakai LY (2010) Biogenesis and function of fibrillin assemblies. *Cell and Tissue Research* **339**, 71–82.

Ramirez F, Sakai LY, Dietz HC, et al. (2004) Fibrillin microfibrils: multipurpose extracellular networks in organismal physiology. *Physiol Genomics* **19**, 151–154.

Rifkin DB (2005) Latent transforming growth factor-beta (TGF-beta) binding proteins: orchestrators of TGF-beta availability. *J Biol Chem* **280**, 7409–7412.

Roaf R. (1960) Vertebral growth and its mechanical control. *J Bone Joint Surg* **42-B**:40–59.

Sakou T, Onishi T, Yamamoto T, et al. (1999) Localization of Smads, the TGF-beta family intracellular signaling components during endochondral ossification. *J Bone Miner Res* **14**, 1145–1152.

Schmid TM, Linsenmayer TF (1985) Immunohistochemical localization of short chain cartilage collagen (type X) in avian tissues. *J Cell Biol* **100**, 598–605.

Sengle G, Charbonneau NL, Ono RN, et al. (2008) Targeting of bone morphogenetic protein growth factor complexes to fibrillin. *J Biol Chem* **283**, 13 874–13 888.

Sengle G, Ono RN, Sasaki T, et al. (2011) Prodomains of transforming growth factor beta (TGFbeta) superfamily members specify different functions: extracellular matrix interactions and growth factor bioavailability. *J Biol Chem* **286**, 5087–5099.

Sengle G, Tsutsui K, Keene DR, et al. (2012) Microenvironmental regulation by fibrillin-1. *PLoS Genet* **8**, e1002425.

Shao YY, Wang L, Ballock RT (2006) Thyroid hormone and the growth plate. *Rev Endocr Metab Disord* **7**, 265–271.

Sherratt MJ, Baldock C, Haston JL, et al. (2003) Fibrillin microfibrils are stiff reinforcing fibres in compliant tissues. *J Mol Biol* **332**, 183–193.

Stokes IA, Gwadera J, Dimock A, et al. (2005) Modulation of vertebral and tibial growth by compression loading: diurnal versus full-time loading. *J Orthop Res* **23**, 188–195.

Stokes IA, Aronsson DD, Dimock AN, et al. (2006) Endochondral growth in growth plates of three species at two anatomical locations modulated by mechanical compression and tension. *J Orthop Res* **24**, 1327–1334.

Stokes IA, Clark KC, Farnum CE, et al. (2007) Alterations in the growth plate associated with growth modulation by sustained compression or distraction. *Bone* **41**, 197–205.

Streeten BW, Licari PA (1983) The zonules and the elastic microfibrillar system in the ciliary body. *Invest Ophthalmol Vis Sci* **24**, 667–681.

Wilsman NJ, Farnum CE, Leiferman EM, et al. (1996) Differential growth by growth plates as a function of multiple parameters of chondrocytic kinetics. *J Orthop Res* **14**, 927–936.

Yamasaki A, Itabashi M, Sakai Y, et al. (2001) Expression of type I, type II, and type X collagen genes during altered endochondral ossification in the femoral epiphysis of osteosclerotic (oc/oc) mice. *Calcif Tissue Int* **68**, 53–60.

Yazaki Y, Matsunaga S, Onishi T, et al. (1998) Immunohistochemical localization of bone morphogenetic proteins and the receptors in epiphyseal growth plate. *Anticancer Res* **18**, 2339–2344.

Yu J, Urban JP (2010) The elastic network of articular cartilage: an immunohistochemical study of elastin fibres and microfibrils. *J Anat* **216**, 533–541.

Yu J, Winlove PC, Roberts S, et al. (2002) Elastic fibre organization in the intervertebral discs of the bovine tail. *J Anat* **201**, 465–475.

Yu J, Tirlapur U, Fairbank J, et al. (2007) Microfibrils, elastin fibres and collagen fibres in the human intervertebral disc and bovine tail disc. *J Anat* **210**, 460–471.